^{89}Y NMR observation of ferromagnetic and antiferromagnetic spin fluctuations in the collapsed tetragonal phase of YFe_{2}(Ge,Si)_{2}

J. Srpčič, P. Jeglič, I. Felner, Bing Lv, C. W. Chu, and D. Arčon

Phys. Rev. B **96**, 174430 — Published 22 November 2017

DOI: 10.1103/PhysRevB.96.174430

^{89}Y NMR observation of ferromagnetic and antiferromagnetic spin fluctuations in the collapsed tetragonal phase of $YFe_2(Ge,Si)_2$

J. Srpčič,[1] P. Jeglič,[1] I. Felner,[2] Bing Lv,[3] C.W. Chu,[4] and D. Arčon[1,5,*]

[1] *Jožef Stefan Institute, Jamova c. 39, 1000 Ljubljana, Slovenia*
[2] *Racah Institute of Physics, The Hebrew University of Jerusalem, Jerusalem, 91904, Israel*
[3] *Department of Physics, The University of Texas at Dallas, Richardson, Texas, 75080-3021, USA*
[4] *Department of Physics and the Texas Center for Superconductivity, University of Houston, Houston, Texas 77204-5005, USA*
[5] *Faculty of Mathematics and Physics, University of Ljubljana, Jadranska c. 19, 1000 Ljubljana, Slovenia*

The surprising discovery of tripling the superconducting critical temperature of KFe_2As_2 at high pressures has led to an intriguing question of how the superconductivity in the collapsed tetragonal phase differs from that in the non-collapsed phases of Fe-based superconductors. Here we report ^{89}Y nuclear magnetic resonance study of $YFe_2Ge_xSi_{2-x}$ compounds whose electronic structure is similar to that of iron-pnictide collapsed tetragonal phases already at ambient pressure. We find that Fe(Ge,Si) layers show ferromagnetic spin fluctuations, whereas the layers are coupled antiferromagnetically. Furthermore, localized moments attributed either to Fe interstitial or antisite defects may account for magnetic impurity pair-breaking effects, thus explaining the substantial variation of superconductivity among different YFe_2Ge_2 samples.

PACS numbers: 76.60.-k, 75.50.Cc, 73.43.Nq, 74.70.Xa

I. INTRODUCTION

The collapsed tetragonal phase (CTP) found in the family of AFe_2As_2 (A = Ba, Ca, Eu, Sr, K) at high pressures has been considered to be a non-superconducting phase[1] because the formation of interlayer As-As bonds triggers topological change of the Fermi surface, thus removing the nesting conditions that are important for superconductivity[2]. This notion was suddenly challenged by the recent discovery of tripling the superconducting critical temperature T_c in KFe_2As_2 at pressures higher than $\sim$ 15 GPa when CTP is formed[3,4]. The strong electron correlations[4] or almost perfectly nested electron and hole pockets found for KFe_2As_2 in CTP[5] were both put forward to explain the surprising enhancement of T_c. Thus, to what degree the superconducting pairing mechanism of CTP differs from that of the non-collapsed layered Fe-based phases[6] remains at present unclear.

Rare earth iron silicides and germanides of the RFe_2X_2 type (R = rare earth element, X = Ge, Si) have been studied since the 1970's for their magnetic properties – various probes showed the absence of the long-range magnetic order of Fe moments in this family of materials[7,8]. The only exception seems to be $LuFe_2Ge_2$, which orders antiferromagnetically with an ordering vector along a [001] direction[9–11]. The two representative compounds YFe_2Si_2 and YFe_2Ge_2 are isostructural to AFe_2As_2, i.e., they all grow in the same body-centered tetragonal crystal structure (Fig. 1a). The ratio of YFe_2Ge_2 tetragonal lattice parameters[12] is $c/a = 2.638$, which is very close to $c/a \approx 2.5$ of the high-pressure CTP in KFe_2As_2[4]. The structural resemblance with CTP of KFe_2As_2 is reflected in the similarities of their electronic structures[5,13–15]. Because of the collapsed tetragonal structure, the interlayer Ge-Ge bonds make the band structure and the Fermi surfaces of YFe_2Ge_2 more three-dimensional[14]. While nesting of hole and electron pockets, similar to that in KFe_2As_2, may further imply that the putative superconductivity in YFe_2Ge_2 has the standard $s_\pm$ order[13], the possible ferromagnetic spin fluctuations within Fe-layers may even promote triplet superconductivity[14]. Reports on experimental observations of superconductivity have been equally controversial. Superconductivity was initially reported for YFe_2Ge_2 below $T_c = 1.8$ K[12]. On the other hand, no bulk superconductivity down to 1.2 K was observed in Ref. 16 and it was argued that the superconductivity has a filamentary nature[17]. However, a more recent study claimed bulk superconductivity in high quality YFe_2Ge_2 ingots with T_c strongly dependent on the sample quality[15].

The key to understanding such conflicting findings is hidden in the normal state of $YFe_2Ge_xSi_{2-x}$ family. First principle calculations[13,14,18] for YFe_2Ge_2 and YFe_2Si_2 suggest that the favorable three-dimensional magnetic order is antiferromagnetic stacking of ferromagnetic Fe-layers along the tetragonal c-axis. However, such long-range antiferromagnetic order has never been experimentally observed for these two compounds despite the enhanced spin susceptibility in the normal state[9,16,19]. The maximum observed in the magnetization measurements across the whole family of $YFe_2Ge_xSi_{2-x}$ has been in some cases interpreted as an indication for a nearly ferromagnetic metal state[16,19], but such maximum could be due to the magnetic impurities. It should be stressed, that the sister $LuFe_2Ge_2$ compound shows the proposed antiferromagnetic ordering at $T_N = 9$ K[9–11] and the complete suppression of T_N by Y substitution on the Lu-site in $Lu_{1-x}Y_xFe_2Ge_2$ for $x \geq 0.2$. This in fact positions $LuFe_2Ge_2$ and YFe_2Ge_2 close to an antiferromagnetic quantum critical point[11–14,16]. Interestingly, strong quantum fluctuations of the Fe spin moments were reported in Refs. 20 and 21. Therefore, if superconduc-

tivity in YFe_2Ge_2 is indeed intrinsic, it develops from a state where strong spin fluctuations probably play an important role in tuning T_c.

Nuclear magnetic resonance (NMR) has been pivotal in studies of iron-based superconductors[22–27] as well as in studies of systems close to the quantum critical point[28–31]. Here, we employ ^{89}Y NMR to probe the normal state of $YFe_2Ge_xSi_{2-x}$ compounds. Data is consistent with the intralayer ferromagnetic and interlayer antiferromagnetic spin fluctuations. $YFe_2Ge_xSi_{2-x}$ is thus laying close to the quantum critical point – the c/a ratio acts as a control parameter to tune the magnetism. Therefore, in tetragonal Fe-based structures with $c/a \sim 2.5$, such as $YFe_2Ge_xSi_{2-x}$ and CTP of KFe_2As_2 or $SrCo_2(Ge_{1-x}P_x)_2$[32], even small perturbations, such as the Fe interstitial or antisite defects discovered in this work, can have a profound effect on the adopted state.

II. EXPERIMENTAL METHODS

A. Sample preparation and characterization

Polycrystalline samples with nominal composition $YFe_2Ge_xSi_{2-x}$ (x = 0.20, 1 and 2), were synthesized by melting stoichiometric amounts of Y, Fe, Si and Ge (all of at least 99.9% purity) in an arc furnace under high-purity Ar atmosphere. All arc-melted buttons were flipped and re-melted several times to ensure homogeneity. The samples were annealed at 850 °C for $\sim$ 100 h and then quenched into liquid nitrogen. Polycrystalline samples were structurally and chemically characterized by a Panalytical X'pert powder x-ray diffraction (XRD) diffractometer. XRD patterns were successfully indexed on the basis of body-centered tetragonal $I4/mmm$-type structure. The lattice parameters previously reported in Ref. 16 are: a = 3.926(1), 3.939(1), 3.966(1) Å and c = 9.974(1), 10.10(1), 10.43(1) Å for x = 0.20, 1 and 2, respectively. The larger Ge size causes both a and c lattice constants to systematically increase with x. As a result, the ratio c/a also smoothly increases with x from 2.54 to 2.63.

Samples were additionally checked for their electrical resistivity properties. The resistivity of YFe_2Ge_2 sample was measured with a conventional four-lead technique using the LR-700 ac resistance bridge between room temperature and 1.2 K. The electrical resistivity, $\rho(T)$ monotonically decreases with decreasing temperature, which is consistent with its metallic nature. The residual resistivity ratio (RRR), is RRR = 19, 8.3 and 8.8 (295/1.3 K) for x = 2, 1 and 0.2 samples, respectively.[16] We note at this point, that according to Ref. 15, YFe_2Ge_2 samples with RRR$\approx$ 20 show superconductivity below $\sim$ 1.3 K, whereas the full resistive transitions with T_c = 1.8 K were observed in most samples with RRR values exceeding 20.

Finally, magnetization measurements in the temperature interval 4.5 K $< T <$ 350 K at various applied fields have been performed using the commercial (Quantum Design) superconducting quantum interference device (SQUID) magnetometer and were previously reported in Ref. 16. Prior to recording the zero-field-cooled (ZFC) curves, the magnetometer was adjusted to be in a true H = 0 state. The magnetization of YFe_2Ge_2 shows a pronounced peak at 75 K (in YFe_2GeSi sample this peak is pushed to lower temperatures),[16] probably originating from some ferromagnetic impurity in our samples. We emphasize at this point, that such parasitic ferromagnetic impurities do not interfere with the ^{89}Y NMR spectra of the dominant $YFe_2Ge_xSi_{2-x}$ phase, because NMR is a local probe technique.

B. NMR measurements

For NMR measurements the samples were crushed to fine powders. The ^{89}Y (nuclear spin I = 1/2) NMR spectra and the spin-lattice as well spin-spin relaxation rates were measured between 5 and 300 K in a magnetic field of 9.4 T. ^{89}Y NMR shifts are determined relative to the Larmor frequency $^{89}\nu_L$ = 19.596 MHz, defined by a Y_2O_3 reference standard. For the ^{89}Y NMR line shape measurements, a Hahn-echo pulse sequence, $\pi/2-\tau-\pi-\tau-$echo, was employed, with a pulse length $t_w(\pi/2) = 11$ μs and an interpulse delay τ = 60 μs. The complete polycrystalline NMR spectrum was obtained by summing the real part of spectra measured step-by-step at resonance frequencies separated by $\Delta\nu$ = 25 kHz. Both, the inversion-recovery and the saturation-recovery pulse sequences were used for the spin-lattice relaxation rate measurements.

III. RESULTS AND DISCUSSION

The ^{89}Y NMR spectrum of $YFe_2Ge_{0.2}Si_{1.8}$, taken at T = 300 K, shows a single line with a characteristic powder pattern of an axially symmetric shift anisotropy (Fig. 1b). Excellent fitting of the spectrum is achieved with the isotropic part of the shift $K_{iso} = (2K_\perp + K_{||})/3 = -0.222\%$ and the shift anisotropy $\delta K = K_\perp - K_{||} = 0.174\%$ ($K_\perp$ and $K_{||}$ are the two principal values of the ^{89}Y NMR shift tensor $\mathbf{K}$). In general, the ^{89}Y NMR shift has two main contributions: the temperature-independent chemical shift and the hyperfine shift. If the dominant contribution to $\mathbf{K}$ arises from the hyperfine, most likely transferred hyperfine, interactions of ^{89}Y with itinerant charges of the Fe(Si,Ge) layer, then from the expression $K_{iso} = \frac{a_{iso}}{N_A\mu_B}\chi$ (N_A and μ_B are the Avogadro number and the Bohr magneton, respectively) we estimate the isotropic hyperfine constant to be $a_{iso} = -6.8$ kOe/μ_B. This is larger than that in, e.g., $YBa_2Cu_3O_{7-y}$ high-T_c superconductors[34,35], by a factor of $\sim$ 4, implying strong coupling of the yttrium layer to the itinerant charges in the electronically active Fe(Ge,Si) layer and consistent with a more three-dimensional band structure[14]. The major uncertainty in

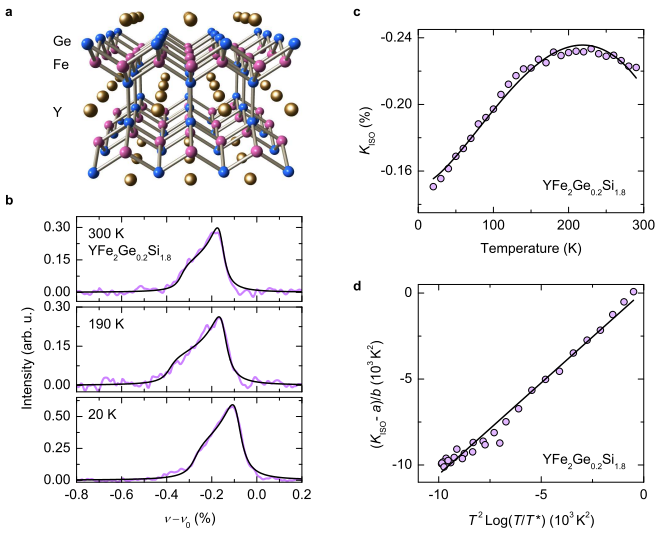

FIG. 1. (color online). (a) The body-centered tetragonal crystal structure of $YFe_2Ge_xSi_{2-x}$ (space group $I4/mmm$). Here small gray, large blue and large pink spheres represent Y, Ge/Si and Fe atoms, respectively. (b) The ^{89}Y NMR spectra (thick violet lines) of polycrystalline $YFe_2Ge_{0.2}Si_{1.8}$ samples at selected temperatures. Solid black line is a fit to uniaxial shift anisotropy. (c) Temperature dependence of ^{89}Y NMR shift, $K_{\rm iso}$ (circles). Solid line is a fit to Eq. (1). (d) Semi-log plot of $K_{\rm iso}$ *vs.* $T^2\ln(T/T^*)$ reveals a straight line thus corroborating intra-plane ferromagnetic correlations.

determining $a_{\rm iso}$ comes from the unknown precise value of the temperature independent chemical shift, which due to the small temperature variations in magnetic susceptibility and the presence of ferromagnetic impurities cannot be reliably determined even from the standard Clogston-Jaccarino plots. We will return to the question of chemical shift latter in connection to the Korringa relation where we estimate it to be $\sim 0.25\%$, which leads to $a_{\rm iso} = -11.6$ kOe/μ_B.

On cooling the ^{89}Y NMR spectra retain their axially symmetric shift anisotropy lineshape at all temperatures (Fig. 1b). The ^{89}Y NMR line first shifts slightly to even more negative values of $K_{\rm iso}$ but then the trend suddenly reverses below $\sim$200 K and the shift, and thus also the local spin susceptibility probed by ^{89}Y, is significantly reduced compared to the room temperature value. The shift anisotropy follows the same trend, e.g., the most shifted spectrum at $T_{\rm max} = 200$ K also has the largest δK. The absence of any significant broadening of ^{89}Y NMR spectra down to $T = 20$ K clearly rules out long-range magnetic ordering in $YFe_2Ge_{0.2}Si_{1.8}$.

$K_{\rm iso}$ thus has a pronounced minimum (or a maximum $|K_{\rm iso}|$) at $T_{\rm max}$ (Fig. 1c), which is marking a maximum in the local spin susceptibility probed by ^{89}Y. Such dependence is markedly different from the monotonic (frequently addressed as a pseudo-gap-like) dependence observed in the iron-pnictide family[22–27]. Moreover, such non-monotonic dependence of χ also strongly deviates from a simple Pauli paramagnetism in metals and is suggestive of spin correlations. The corrections to the temperature dependence of the spin susceptibility of normal paramagnetic metals in the presence of ferromagnetic spin fluctuations have been a subject of intense theoretical discussions[36–39]. The maximum in $\chi(T)$ is predicted when the spin susceptibility is given by

$$\chi(T) = \chi(0) - bT^2\ln(T/T^*)\,, \qquad (1)$$

where $\chi(0)$ is the Pauli spin susceptibility (which is modified by enhancement factor S) and T^* reflects the cutoff energies, whereas prefactor b is also strongly dependent on the enhancement factor, i.e., $b \propto S^4$. If we insert Eq. (1) into the expression for $K_{\rm iso}$ and use $a_{\rm iso} = -11.6$ kOe/μ_B, we obtain a high $\chi(0) = 1.5(1)\cdot10^{-3}$ emu/mol, $b = 3.6(2)\cdot10^{-7}$ emu/(mol K^2) and $T^* = 351(2)$ K. The agreement with the model is further demonstrated on a semi-log plot of $K_{\rm iso}$ *vs* $T^2\ln(T/T^*)$, where all experimental points fall on a straight line (Fig. 1d), thus giving a support for the intra-plane ferromagnetic fluctuations in $YFe_2Ge_{0.2}Si_{1.8}$. However, the high Sommerfeld ratio $\gamma \sim 100$ mJ/(molK^2)[15] suggest that both heat capacity and spin susceptibility are enhanced by the same factor of ~ 10 compared to their unrenormalized values, meaning that the Wilson ratio χ_0/γ is of the order of 1, which would not appear to support the nearly ferromagnetic state.

Partial or complete replacement of Si with Ge yields isostructural YFe_2GeSi and YFe_2Ge_2 compositions. Compared to $YFe_2Ge_{0.2}Si_{1.8}$, the ^{89}Y NMR spectrum of YFe_2GeSi is significantly broader and shifted to even lower resonance frequencies (Fig. 2a). The broadening is attributed to the effects of local site disorder introduced by a random Si and Ge occupancy of 4*e* crystallographic positions. On the other hand, since it is unlikely that the structural and electronic modifications within the Fe(Ge,Si) layer would considerably affect the values of ^{89}Y hyperfine constant $a_{\rm iso}$ the observed monotonic increase of the ^{89}Y shift with increasing Ge content can only reflect the enhancement of local spin susceptibilities. The ^{89}Y NMR spectrum of YFe_2Ge_2 (Fig. 2b) is shifted even more, thus implying even larger local spin susceptibilities probed by ^{89}Y NMR.

^{89}Y NMR spectra retain their axially symmetric shift anisotropy lineshape at all temperatures (Fig. 2), hence indicating that there is no structural phase transition between 300 and 15 K that would reduce the ^{89}Y 2*a* site symmetry in either sample. Compared to $YFe_2Ge_{0.2}Si_{1.8}$, the temperature $T_{\rm max}$, where $K_{\rm iso}$ reaches its minimum (maximum in $|K_{\rm iso}|$), is systematically reduced with increasing Ge content (Fig. 3a), i.e. to ~ 100 K and ~ 70 K in YFe_2GeSi and YFe_2Ge_2 samples (inset to Fig. 3b), respectively. Moreover, fitting of the temperature dependences of $K_{\rm iso}$ to Eq. 1 is no longer satisfactory. Even extensions of a model to include effects of impurities[39], i.e., $\chi(T) = \chi(0) - bT^2\ln[(T + T_{\rm imp})/T^*]$, where $T_{\rm imp}$ is related to the effects of the finite mean free path on the spin fluctuations, do not improve the quality of the

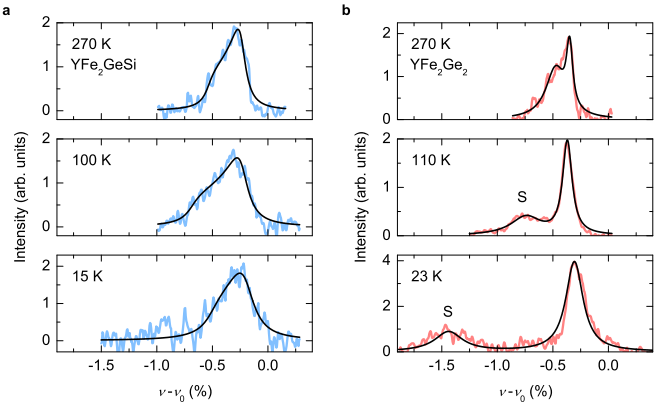

FIG. 2. (color online). ^{89}Y NMR spectra of (a) YFe_2GeSi and (b) YFe_2Ge_2 shown for some selected temperatures. Thick lines represent the experimental data, while thinner solid lines are lineshape fits. The label S marks the position of additional strongly shifted ^{89}Y line attributed to those Y ions, which couple to localized moments. These moments are associated with the Fe creating antisites or interstitial defects.

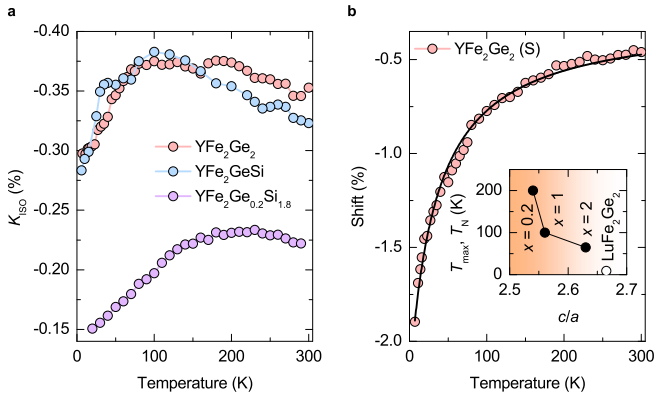

FIG. 3. (color online). (a) Comparison of temperature dependences of the isotropic part of the ^{89}Y NMR shifts K_{iso} measured for $YFe_2Ge_{0.2}Si_{1.8}$ (violet), YFe_2GeSi (blue) and YFe_2Ge_2 (red) powders. (b) The shift of the additional ^{89}Y resonance (circles), with the signal intensity of about 20% of the total NMR signal, follows a Curie-like temperature dependence (solid line). Inset: The dependence of temperature T_{max}, i.e., the temperature where $|K_{iso}|$ has a maximum for the $YFe_2Ge_xSi_{2-x}$ family, on the c/a ratio (solid circles). The open circle represents $T_N = 9$ K of $LuFe_2Ge_2$[9].

fit. Contrary to $YFe_2Ge_{0.2}Si_{1.8}$, the ^{89}Y NMR spectra remain broad when $|K_{iso}|$ is reduced at low temperatures (e.g., compare the spectra of YFe_2Ge_2 measured at 110 and 23 K in Fig. 2b). This is indicative of the growth of local magnetic fields at ^{89}Y sites probably originating from the short-range static magnetic correlations that begin to develop in a high magnetic field of 9.34 T at low temperatures. It should be noted that $|K_{iso}|$ is suppressed at the lowest temperatures, which necessitates that correlations between the Fe(Si,Ge) layers are of antiferromagnetic nature.

Another peculiarity of the YFe_2Ge_2 sample is a pronounced shoulder in the ^{89}Y NMR spectra, which on cooling develops into a separate resonance with an extremely large shift (Fig. 2b). This spectral component is absent (or at least much weaker) in the other two compounds. Since all three studied samples grow in the same space group with a single crystallographic Y site, there is no obvious reason for a separate ^{89}Y NMR line in this case. The intensity of this signal is about 20% of the total ^{89}Y NMR signal so it cannot be simply attributed to some extrinsic ferromagnetic impurity phase, leading us to the conclusion that it must be intrinsic to YFe_2Ge_2. The temperature dependence of the shift (Fig. 3b) follows a perfect Curie-Weiss behaviour, i.e. $K^s_{iso} = K_0 + C/(T - T_0)$ with $K_0 = -1890$ ppm, $C = -0.89$ K and $T_0 = -48$ K, thus associating this signal with ^{89}Y sites located close to some localized moments. This notion is further supported by the measurements of the spin-lattice relaxation rate, $1/T_1$, which is, for this component, nearly temperature independent (Fig. 4a). To explain the presence of localized paramagnetic impurities, we refer here to a common feature also frequently encountered in iron-pnictide and iron-chalcogenide samples[26,40,41], i.e., that some of the Fe creates antisites (Fe occupying Ge/Si sites) or interstitial defects (Fe occupying crystallographic interstitial sites between Y and Ge layers). Due to the large magetic moment of such localized Fe defects, a strong hyperfine field with a Curie-Weiss-like dependence is anticipated on the nearest neighboring ^{89}Y sites, in agreement with the experiment. We note that the presence of such localized moments may account for the variations in RRR between different samples and provide a very efficient channel for magnetic impurity pair-breaking effects, thus explaining the large variation in T_c for different YFe_2Ge_2 samples[12,15–17].

Strong quantum spin fluctuations are usually responsible for a characteristic power-law dependence of the spin-lattice relaxation rate, $1/T_1$, i.e., $1/T_1T \propto T^{-n}$ with $n = 3/4$.[28–31] However, for $YFe_2Ge_xSi_{2-x}$, the respective ^{89}Y spin-lattice relaxation rates divided by temperature, $1/T_1T$, do not show such dependence (Fig. 4a). A detailed analysis of the contributions of different **q**-dependent spin fluctuations to the ^{89}Y spin-lattice relaxation would require also a detailed information about the ^{89}Y hyperfine tensor. Moreover, much of the information about the resulting anisotropy in $1/T_1$ is lost in measurements on powder samples. However, even the discussion of the simple Korringa relaxation relation[25] may hold important clues about the dominant type of spin fluctuations observed at the ^{89}Y site. In connection to that we note that for $YFe_2Ge_{0.2}Si_{1.8}$ the temperature dependence of $1/T_1T$ resembles that of K_{iso}, i.e., it exhibits a broad maximum at ~ 200 K. When the electron-electron exchange enhancement effects are important, the Korringa

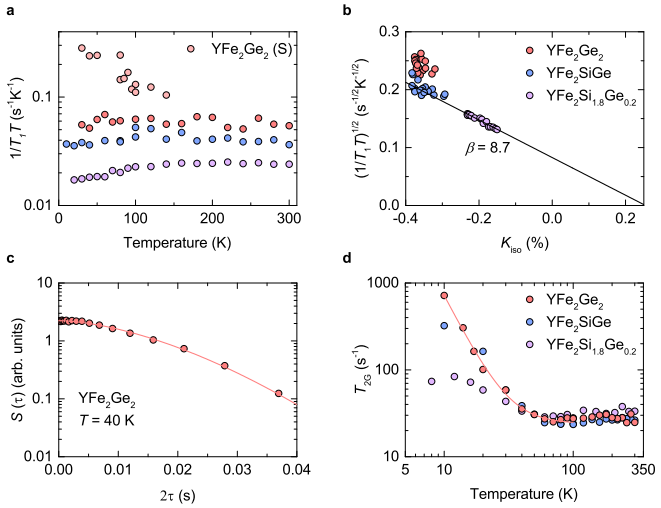

FIG. 4. (color online). (a) Temperature dependences of ^{89}Y spin-lattice relaxation rates $1/T_1T$ for $YFe_2Ge_xSi_{2-x}$ samples. (b) Test of the Korringa relation for $YFe_2Ge_xSi_{2-x}$ samples by plotting $\sqrt{1/T_1T}$ *vs.* $K_{\rm iso}$ with temperature as an implicit parameter. The solid black line is the Korringa relation (Eq. 2) yielding the Korringa factor $\beta = 8.7$. (c) The decay of echo signal intensity as a function of interpulse delay time τ measured in YFe_2Ge_2 at $T = 40$ K. The solid line is a fit with $\alpha = 1.65$ (see text for details). (d) Temperature dependences of Gaussian spin-spin relaxation rates $1/T_{2G}$. Solid red line is a fit for YFe_2Ge_2 to a low-temperature power-law T^{-n} dependence with $n = 2.9(1)$. The labeling of different samples is provided in insets.

relation reads[42]

$$T_1TK_{\rm iso}^2 = \frac{\hbar}{4\pi k_{\rm B}}\frac{\gamma_{\rm e}^2}{\gamma_{89}^2}\beta\,. \qquad (2)$$

Here $\gamma_{\rm e}$ and γ_{89} are the electronic and ^{89}Y gyromagnetic ratios, respectively. The Korringa factor β is introduced to account for the electron-electron exchange in a strongly correlated metal[42]. Plotting $\sqrt{1/T_1T}$ *vs.* $K_{\rm iso}$, we find the expected linear dependence (Fig. 4b) yielding $\beta = 8.7$, with line intercepting the horizontal axis at 0.25%. Moreover, adding to the same plot also the data from the YFe_2GeSi sample, then the data points from both samples fall on the same line, thus strengthening our estimate of β and placing 0.25% as a reliable estimate of the chemical shift. Such enhancement in β is consistent with the previously established intra-plane ferromagnetic spin fluctuations. The spin-lattice relaxation rates of YFe_2Ge_2 are even more enhanced, nearly temperature independent (Fig. 4a) and do not scale with the temperature dependent $K_{\rm iso}^2$ (Fig. 3a), giving indications for a Fermi-liquid breakdown for this sample.

In the $BaFe_2As_2$ family, where the coexistence of the intra-plane ferromagnetic and stripe-type antiferromagnetic spin correlations was recently reported[23,27], $1/T_1T$ increases with decreasing temperature, because of the contribution of the dynamic spin susceptibility at the antiferromagnetic wave-number $\mathbf{Q}$, which increases with decreasing temperature. Since such characteristic enhancement is not observed in our $1/T_1T$ data, we conclude that for the $YFe_2Ge_xSi_{2-x}$ family the intra-plane ferromagnetic fluctuations prevail over the intra-plane stripe-type antiferromagnetic fluctuations at all temperatures. However, since the temperature dependence of $K_{\rm iso}$ at the lowest temperatures indicate also antiferromagnetic correlations, this brings us to the antiferromagnetic coupling between layers, which was initially found in the first principle calculations[13,14,18] and in the antiferromagnetic ordering of the sister $LuFe_2Ge_2$ compound[9]. The inter-plane antiferromagnetic spin fluctuations are in the $1/T_1T$ data, however, filtered out at the highly symmetric yttrium position. To address antiferormagnetic correlations between layers we finally turn to ^{89}Y spin-spin relaxation rates, $1/T_2$. We first fitted the envelope of the echo decay $S(\tau)$ as a function of the interpulse delay time τ to a phenomenological expression $S(\tau) = S_0\exp[-(2\tau/T_2)^{\alpha}]$ (Fig. 4c). Here S_0 is the initial echo intensity signal, whereas the parameter α expresses the relative contributions of the Redfield and the Gaussian parts of the echo decay[42,43]. We obtain $\alpha \approx 1.6$, showing that both relaxation channels are present and comparable. Therefore, in the next step we employed the procedure of Ref. 43 to extract the Gaussian part of the decay, T_{2G}. As anticipated, $1/T_{2G}$ is constant at high temperatures for all samples (Fig. 4d). However, at low temperatures, $1/T_{2G}$ nearly diverges for YFe_2Ge_2 and YFe_2GeSi, whereas it is only slightly enhanced for $YFe_2Ge_{0.2}Si_{1.8}$. Below 100 K, $1/T_{2G}$ for YFe_2Ge_2 is fitted to $1/T_{2G} = 1/T_2^0 + BT^{-n}$ with a power exponent $n = 2.9(1)$. This is reminiscent of cuprates, where the Gaussian contribution to the echo decay is proportional to the antiferromagnetic correlation length ξ, i.e., $1/T_{2G} \propto \xi$[42–45]. The low-temperature enhancement in $1/T_{2G}$ thus corroborates the growth of antiferromagnetic correlations between Fe(Ge,Si) layers and suggests that the Ge-rich samples are in the vicinity of an antiferromagnetic quantum critical point.

IV. CONCLUSIONS

The $YFe_2Ge_xSi_{2-x}$ family displays ferromagnetic fluctuations within the Fe(Ge,Si) layers and antiferromagnetic correlations between layers. These latter grow in importance with $x \to 2$, thus implying that with the introduction of slightly larger Ge ions, the change in the c/a ratio ($c/a = 2.54$, 2.56 and 2.63 for $x = 0.2, 1$ and 2 samples, respectively) is sufficient to strengthen the interlayer coupling. The trend is in agreement with the long range antiferromagnetic order below 9 K in $LuFe_2Ge_2$ ($c/a = 2.66$)[9] and the smooth suppression of $T_{\rm N}$ in $Lu_{1-x}Y_xFe_2Ge_2$ as Y partially replace Lu.[11] YFe_2Ge_2 is close to the antiferromagnetic quantum critical point (inset to Fig. 3b). We stress that a similar Ge-Ge bonding strength acting as a tuning parameter to in-

duce the quantum critical point has been reported for $SrCo_2(Ge_{2-x}P_x)_2$, which likewise belongs to the same layered tetragonal $ThCr_2Si_2$ structure type[32]. When a quantum critical point separates the magnetic and superconducting phases, even small perturbations introduced by defect localized moments, such as those reported here, may have a profound effect on the ground state. Although there is no NMR data available for a comparison with the high-pressure CTP phase of KFe_2As_2, our results suggest some important differences, most notably ferromagnetic intra-plane fluctuations, in the normal state of $YFe_2Ge_xSi_{2-x}$ compared to that of the superconducting iron-pnictides. It is therefore unlikely that superconductivity in YFe_2Ge_2 follows the same scenarios as those discussed for iron-pnictides[6].

D.A. acknowledges the financial support by the Slovenian Research Agency, grant No. N1-0052. B. L and C. W. C acknowledge the financial support by US Air Force Office of Scientific Research Grants No. FA9550-15-1-0236.

* e-mail: denis.arcon@ijs.si

[1] D. K. Pratt, Y. Zhao, S. A. J. Kimber, A. Hiess, D. N. Argyriou, C. Broholm, A. Kreyssig, S. Nandi, S. L. Bud'ko, N. Ni, et al., Phys. Rev. B **79**, 060510 (2009).

[2] A. I. Coldea, C. M. J. Andrew, J. G. Analytis, R. D. McDonald, A. F. Bangura, J.-H. Chu, I. R. Fisher, and A. Carrington, Phys. Rev. Lett. **103**, 026404 (2009).

[3] Y. Nakajima, R. Wang, T. Metz, X. Wang, L. Wang, H. Cynn, S. T. Weir, J. R. Jeffries, and J. Paglione, Phys. Rev. B **91**, 060508 (2015).

[4] J.-J. Ying, L.-Y. Tang, V. V. Struzhkin, H.-K. Mao, A. G. Gavriliuk, A.-F. Wang, X.-H. Chen, and C. Xiao-Jia, arXiv:1501.00330 **(unpublished)** (2015).

[5] D. Guterding, S. Backes, H. O. Jeschke, and R. Valentí, Phys. Rev. B **91**, 140503 (2015).

[6] H. Hosono and K. Kuroki, Physica C **514**, 399 (2015).

[7] I. Felner, I. Mayer, A. Grill, and M. Schieber, Solid State Commun. **16**, 1005 (1975).

[8] H. Pinto and H. Shaked, Phys. Rev. B **7**, 3261 (1973).

[9] M. Avila, S. Bud'ko, and P. Canfield, J. Magn. Magn. Mater. **270**, 51 (2004).

[10] T. Fujiwara, N. Aso, H. Yamamoto, M. Hedo, Y. Saiga, M. Nishi, Y. Uwatoko, and K. Hirota, Journal of the Physical Society of Japan **76**, 60 (2007).

[11] S. Ran, S. L. Bud'ko, and P. C. Canfield, Philosophical Magazine **91**, 4388 (2011).

[12] Y. Zou, Z. Feng, P. W. Logg, J. Chen, G. Lampronti, and F. M. Grosche, physica status solidi **8**, 928 (2014).

[13] A. Subedi, Phys. Rev. B **89**, 024504 (2014).

[14] D. J. Singh, Phys. Rev. B **89**, 024505 (2014).

[15] J. Chen, K. Semeniuk, Z. Feng, P. Reiss, P. Brown, Y. Zou, P. W. Logg, G. I. Lampronti, and F. M. Grosche, Phys. Rev. Lett. **116**, 127001 (2016).

[16] I. Felner, B. Lv, K. Zhao, and C. W. Chu, J. Supercond. Nov. Magn. **28**, 1207 (2015).

[17] H. Kim, S. Ran, E. Mun, H. Hodovanets, M. Tanatar, R. Prozorov, S. Budko, and P. Canfield, Philos. Mag. **95**, 804 (2015).

[18] D. J. Singh, Phys. Rev. B **93**, 245155 (2016).

[19] I. Felner, B. Lv, and C. W. Chu, J. Phys. – Condens. Mat. **26**, 476002 (2014).

[20] N. Sirica, F. Bondino, S. Nappini, I. Píš, L. Poudel, A. D. Christianson, D. Mandrus, D. J. Singh, and N. Mannella, Phys. Rev. B **91**, 121102 (2015).

[21] J. Ferstl, H. Rosner, and C. Geibel, Physica B **378 – 380**, 744 (2006).

[22] G. R. Stewart, Rev. Mod. Phys. **83**, 1589 (2011).

[23] D. C. Johnston, Adv. Phys. **59**, 803 (2010).

[24] P. Jeglič, J.-W. G. Bos, A. Zorko, M. Brunelli, K. Koch, H. Rosner, S. Margadonna, and D. Arčon, Phys. Rev. B **79**, 094515 (2009).

[25] P. Jeglič, A. Potočnik, M. Klanjšek, M. Bobnar, M. Jagodič, K. Koch, H. Rosner, S. Margadonna, B. Lv, A. M. Guloy, et al., Phys. Rev. B **81**, 140511 (2010).

[26] M. Majcen Hrovat, P. Jeglič, M. Klanjšek, T. Hatakeda, T. Noji, Y. Tanabe, T. Urata, K. K. Huynh, Y. Koike, K. Tanigaki, et al., Phys. Rev. B **92**, 094513 (2015).

[27] P. Wiecki, B. Roy, D. C. Johnston, S. L. Bud'ko, P. C. Canfield, and Y. Furukawa, Phys. Rev. Lett. **115**, 137001 (2015).

[28] T. Moriya and T. Takimoto, J. Phys. Soc. Jpn. **64**, 960 (1995).

[29] A. Ishigaki and T. Moriya, J. Phys. Soc. Jpn. **65**, 3402 (1996).

[30] R. Sarkar, P. Khuntia, C. Krellner, C. Geibel, F. Steglich, and M. Baenitz, Phys. Rev. B **85**, 140409 (2012).

[31] T. Misawa, Y. Yamaji, and M. Imada, J. Phys. Soc. Jpn. **78**, 084707 (2009).

[32] S. Jia, P. Jiramongkolchai, M. R. Suchomel, B. H. Toby, J. G. Checkelsky, N. P. Ong, and R. J. Cava, Nat. Phys. **7**, 207 (2011).

[33] T. Aharen, J. E. Greedan, C. A. Bridges, A. A. Aczel, J. Rodriguez, G. MacDougall, G. M. Luke, T. Imai, V. K. Michaelis, S. Kroeker, et al., Phys. Rev. B **81**, 224409 (2010).

[34] M. Takigawa, W. L. Hults, and J. L. Smith, Phys. Rev. Lett. **71**, 2650 (1993).

[35] H. Alloul, A. Mahajan, H. Casalta, and O. Klein, Phys. Rev. Lett. **70**, 1171 (1993).

[36] M. T. Béal-Monod, S.-K. Ma, and D. R. Fredkin, Phys. Rev. Lett. **20**, 929 (1968).

[37] S. Misawa, Phys. Lett. A **32**, 153 (1970).

[38] G. Barnea, J. Phys. C Solid State **8**, L216 (1975).

[39] G. Barnea, J. Phys. F Met. Phys. **7**, 315 (1977).

[40] H. Sun, D. N. Woodruff, S. J. Cassidy, G. M. Allcroft, S. J. Sedlmaier, A. L. Thompson, P. A. Bingham, S. D. Forder, S. Cartenet, N. Mary, et al., Inorg. Chem. **54**, 1958 (2015).

[41] U. Pachmayr, F. Nitsche, H. Luetkens, S. Kamusella, F. Brckner, R. Sarkar, H.-H. Klauss, and D. Johrendt, Angew. Chem. Int. Edit. **54**, 293 (2015).

[42] R. E. Walstedt, *The NMR Probe of High-Tc Materials*, vol. 228 of *Springer Tracts in Modern Physics* (Springer Berlin Heidelberg, 2008).

[43] N. J. Curro, T. Imai, C. P. Slichter, and B. Dabrowski, Phys. Rev. B **56**, 877 (1997).

[44] V. Barzykin and D. Pines, Phys. Rev. B **52**, 13585 (1995).

[45] C. H. Pennington and C. P. Slichter, Phys. Rev. Lett. **66**, 381 (1991).